Formation of plasma ionization state in the course of evaporation by a laser

I. B. Levinson, A. E. Kramida, G. V. Pereguda, E. N. Rogozin, and V. A. Chirkov

P. N. Lebedev Physics Institute, USSR Academy of Sciences

The plasma produced when a solid target is evaporated by a laser is located in a stationary layer (of the Knudsen type) adjacent to the target. The boundary of this layer in the nonstationary flow region (the jet itself) is the Jouguet point. Under the assumptions indicated, a theory of the stationary layer is presented and the boundary condition for the jet, namely the connection between the electron temperature and the degree of ionization at the Jouguet point, is obtained. The dependence of these parameters on the gasdynamic flow in the jet is obtained. A comparison with experiment is made.

PACS numbers: 52.50.Jm, 52.30. + r, 47.55.Cy

When a solid target is irradiated by a laser of sufficient intensity, the radiation is absorbed not by the target itself, but in a layer of dense ionized plasma produced near the target surface. The problem of target evaporation under such conditions was solved in Ref. 1, where it was assumed that the degree of plasma ionization is given. The evolution of the ionization in the course of evaporation was considered, e.g. in Ref. 2, where a self-similar solution was obtained for the expanding plasma.

It is known[3] that in ordinary evaporation the self-similar solution is established outside the Knudsen layer located near the evaporating surface, and the flow in this layer is stationary regardless of the evaporation regime. It is natural to assume that a stationary layer of this kind should exist also in the case of laser evaporation. Its investigation is in fact the purpose of the present paper.

We consider a planar target (located at $x < 0$) and assume, just as in Ref. 1, that all the radiation is absorbed in a point $x_* = 0$, where the electron density $n_e(x)$ is equal to the critical value n_*. We neglect the absorption in the more rarefield jet. In addition, we assume that the flow in the region $0 < x < x_*$ is stationary and that x_* is the Jouguet point (i.e., the hydrodynamic velocity at the point x_* is equal to the local isothermal sound velocity). We note that the existence of a stationary layer with such properties was noted in Ref. 1 for a planar geometry and a fixed degree of ionization.

The stationary region $x < x_*$ can be regarded as the region of plasma formation, while the nonstationary region $x > x_*$, where the plasma is described, e.g., by a refraction wave, as the plasma-jet region. We shall focus our attention on the formation regions, and determine how the electron temperature $T_e(x)$ is connected with the degree $z(x)$ of plasma ionization at the point x_*. This connection is the boundary condition for the solution of the problem of plasma expansion in the jet region.

1. IONIZATION, RECOMBINATION, AND THERMAL CONDUCTIVITY

The physical processes that occur in the plasma-formation region are determined by ionization, recombination, and thermal conductivity.

According to Ref. 4, the rate of the ionization $l^m \rightarrow l^{m-1}$ (m is the number of equivalent electrons in the outer electron shell of the ion) is

$$S_z(T_e) = 10^{-8} \frac{m}{2l+1} \left(\frac{E_z}{\text{Ry}} \right)^{-3/2} e^{-\beta} \frac{A\beta^{1/2}}{\beta+a} \ [\text{cm}^3/\text{sec}]. \quad (1.1)$$

Here E_z is the ionization potential, $\beta = E_z/T_e$, A and a are constants, and l is the angular momentum of the outer-shell electron.

The rate of the photorecombination $l^{m-1} \rightarrow l^m$ is expressed as follows:

$$\alpha_z(T_e) = 10^{-14} \frac{4l+3-m}{4l+2} \left(\frac{E_z}{\text{Ry}} \right)^{1/2} \frac{B\beta^{3/2}}{\beta+b}, \quad (1.2)$$

where B and b are constants.

In the analytic calculations we shall replace m by its mean value $\bar{m} = 2l + 1$ and approximate the dependence of the ionization potential on the degree of ionization by a power-law function:

$$E_z = E_0(z+1)^k. \quad (1.3)$$

The constants E_0 and k, as incidentally also the constants A, a, B, and b, are different for different shells. The quantity of interest to us

$$\gamma_z(T_e) = S_z(T_e) - \alpha_z(T_e) \quad (1.4)$$

can then be written in the form

$$\gamma_z(T_e) = S_0 \left(\frac{T_e}{E_0} \right)^{-1/2} z^{-k} \left\{ \frac{e^{-\beta}}{\beta+a} - r z^{2k} \frac{\beta}{\beta+b} \right\}. \quad (1.5)$$

Here

$$S_0 = 10^{-8} \bar{m} \frac{A}{2l+1} \left(\frac{E_0}{\text{Ry}} \right)^{-3/2}, \quad (1.6)$$

$$r = 10^{-6} \left(\frac{E_0}{\text{Ry}} \right)^2 \frac{l+1}{2l+1} \frac{B}{A}. \quad (1.7)$$

The constant quantities E_0, k, and S_0 for ions with different outer electron shells are listed in Table I. The headings $2s$—$2p$ in this table pertain to ions with ground state configurations $1s^2 2s^m$ ($m = 1 - 2$) and $1s^2 2s^2 2p^m$ ($m = 1 - 6$), and

TABLE I.

	Ca		Ti		
	$2s{-}2p$	$3s{-}3p$	$2s{-}2p$	$3s{-}3p$	$+\frac{2s-2p}{3s-3p}$
E_0, eV	20.85	13.03	21.33	12.95	0.22
k	1.39	1.19	1.40	1.24	3.2
S_0, 10^{-7} cm$^{-3}\cdot$sec^{-1}	1.58	3.20	1.53	3.23	1460
M, 10^{-22} g	0.665		0.795		
$\varkappa_0$, 10^{24} cm$^{-1}\cdot$sec^{-1}	3.19	0.98	3.38	0.97	0.000035
$\lambda/10^5$	3.34		4.00		
W_0, 10^9 W$\cdot$cm^{-2}	7.10	3.51	6.72	3.18	0.007
z_{max}	17	9	19	11	19
z_{min}	10	2	12	4	4

	Fe		Ni		Cu	
	$2s{-}2p$	$3s{-}3p$	$2s{-}2p$	$3s{-}3p$	$2s{-}2p$	$3s{-}3p$
E_0, eV	22.53	13.48	22.97	13.75	23.17	13.85
k	1.42	1.29	1.43	1.30	1.43	1.31
S_0, 10^{-7} cm$^{-3}\cdot$sec^{-1}	1.41	3.04	1.37	2.95	1.35	2.92
M, 10^{-22} g	0.927		0.974		1.05	
$\varkappa_0$, 10^{24} cm$^{-1}\cdot$sec^{-1}	3.87	1.07	4.07	1.13	4.16	1.15
$\lambda/10^5$	4.66		4.90		5.28	
W_0, 10^9 W$\cdot$cm^{-2}	6.76	3.13	6.79	3.14	6.62	3.06
z_{max}	23	15	25	17	26	18
z_{min}	16	8	18	10	19	11

$3s - 3p$ to the configurations $1s^2 2s^2 2p^6 3s^m$ ($m = 1 - 2$) and $1s^2 2s^2 2p^6 3s^2 3p^m$ ($m = 1 - 6$). The values of E_0 and k were determined by least-squares averaging of the ionization potentials cited in Ref. 5. For Ca and Ti we have also constructed a single continuous function that approximates the dependence of the ionization rate on the ion charge for the $2s$–$2p$ and $3s$–$3p$ shells jointly. The parameters E_0, k, and S_0 were determined with the aid of this function. Their values for Ti are given in Table I in the column headed $(2s - 2p) + (3s - 3p)$, and for Ca in Table III below. In this case, the dependence of the ionization potential on the ion charge, $E_z = E_0(z + 1)^k$, is approximate. This dependence, however, enters in the theory only via the ionization rate, so that this manner of specifying $E_z(z)$ allows us to use the theory parameters E_0, k, and S_0 without incurring appreciable errors. The close values of e^{β_*} for both approximations (see, e.g., Table III) mean that consideration of two shells results in an error that at any rate is not larger than the case of one shell. At the same time, the accuracy obtained thereby is higher, since the ionization can be taken into account during its earlier stages. The quantities z_{max} and z_{min} describe the limits of the variation of the ionization multiplicities z, between which an approximation with given definite parameters E_0 and k is valid.

We turn now to the thermal conductivity. According to Ref. 6, the reciprocal thermal-conductivity coefficient is

$$\frac{1}{\varkappa} = \frac{m_e}{n_e T_e} \frac{1}{\tau_{ei}} = \frac{m_e}{n_e T_e} \sum_z n_z \langle v_e \sigma_{ei}^z \rangle. \tag{1.8}$$

Here m_e is the electron mass, n_e is the electron density, τ_{ei} is the time of electron scattering by the ions, σ_{ei}^z is the cross section for this scattering by ions with charge z, and n_z is the

density of these ions. Since $\sigma_{ei}^z = z^2 \sigma_{ei}^1$, we can express in the form

$$\frac{1}{\varkappa} = \frac{m_e}{T_e} \langle v_e \sigma_{ei}^1 \rangle \frac{\overline{z^2}}{\bar{z}}, \tag{1.9}$$

where the mean values are

$$\overline{z^2} = \frac{1}{n_i} \sum_z z^2 n_z, \quad \bar{z} = \frac{1}{n_i} \sum_z z n_z, \quad n_i = \sum_z n_z, \tag{1.10}$$

and n_i is the total density of the heavy particles. By expression n_e in (1.8) in terms of $\bar{z}$, we have taken into account the neutrality condition

$$n_e = \sum_z z n_z = \bar{z} n_i. \tag{1.11}$$

If we assume approximately $\overline{z^2} = \bar{z}^2$, we can write for $\varkappa$

$$\varkappa = \varkappa_0 \bar{z}^{-1} (T_e/E_0)^{5/2}, \tag{1.12}$$

where $\varkappa_0$ is the thermal conductivity at $\bar{z} = 1$ and $T_e = E_0$ (see Table I).

2. BASIC EQUATIONS OF STATIONARY LAYER

In the derivation of the equations of plasma motion and ionization in the region of the plasma formation we shall assume that all the plasma components have the same drift velocity u. Together with the neutrality condition (1.11) this ensures the absence of electric currents. We consider first the mass, momentum, and energy transport equations:

The mass conservation law:

$$\frac{d}{dx} \rho u = 0, \quad \rho = M n_i, \tag{2.1}$$

where ρ is the density and M the mass of the heavy particle; we neglect the electron mass.

The momentum conservation law:

$$\rho u \frac{du}{dx} + \frac{dp}{dx} = 0, \quad p = n_e T_e + \sum_z n_z T_i^z. \tag{2.2}$$

Here p is the pressure and T_i^z is the kinetic temperature of ions with charge z. Since the ions are heated only by the electrons, $T_i^z < T_e$. At the same time, at a high degree of plasma ionization we have $n_e \gg n_i$. We can therefore neglect the ion pressure and put $p = n_e T_e$.

The energy conservation law:

$$\frac{d}{dx}\left\{ \rho u \left[\frac{u^2}{2} + \frac{\gamma}{\gamma-1} \frac{p}{\rho} \right] - \varkappa \frac{dT_e}{dx} \right\} = 0, \tag{2.3}$$

where $\gamma > 5/3$ is the effective adiabatic exponent that takes the energy loss to ionization into account.

Equations (2.1)–(2.3) contain the following unknown functions: u, n_i, n_e, and T_e. The thermal conductivity depends according to (1.12) on $\bar{z}$ and T_e. Noting that $n_i = n_e/\bar{z}$, it is convenient to choose the functions u, n_e, T_e, and z as the unknowns. It is now clear that we are lacking one equation. To derive it we write down the electron-number balance. We note for this purpose that in electron-impact ionization processes $z \to z + 1$ each electron has a probability S_z of "creating" one more electron, while in photorecombination $z \to z - 1$ an electron z has an "annihilation" probability α_z. Therefore, using the definition (1.4), we have

$$\frac{d}{dx} n_e u = n_e \sum_z n_z \gamma_z. \tag{2.4}$$

Introducing the mean values (1.10), we write approximately

$$\sum_z n_z \gamma_z = \gamma_{\bar{z}} \sum_z n_z. \tag{2.5}$$

We then obtain the missing fourth equation

$$\frac{d}{dx} n_e u = \frac{\gamma_{\bar{z}}}{\bar{z}} n_e^2. \tag{2.6}$$

We now rewrite all four equations in terms of the chosen variables, simplifying the notation: $\bar{z} \to z$, $T_e \to T$, $n_e \to n$. From (2.1) and (2.2) we have

$$\frac{d}{dx} \frac{nu}{z} = 0, \tag{2.7}$$

$$\frac{d}{dx}\left[M \frac{nu^2}{z} + nT \right] = 0. \tag{2.8}$$

Using (2.7), we can rewrite (2.6) as

$$\frac{dz}{dx} = \frac{n}{u} \gamma_{\bar{z}}(z, T). \tag{2.9}$$

If we neglect the energy flux into the target, the total energy flux (thermal + gasdynamic) is zero, and (2.3) takes the form

$$\frac{dT}{dx} = \frac{Mnu}{z\varkappa(z,T)}\left[\frac{1}{2} u^2 + \frac{\gamma}{\gamma-1} z \frac{T}{M} \right]. \tag{2.10}$$

Equations (2.7)–(2.10) constitute the complete system of equations for the variables u, n, z, and T.

The plan for solving these equations is the following. We specify the values of z and T at the point $x = x_*$ and designate them z_* and T_*. We know the value n_* of n at the point x. The velocity u_* at this point can be expressed in terms of z_* and T_*, inasmuch as by assumption x_* is the Jouguet point:

$$u_*^2 = (1 + z_*) T_*/M \approx z_* T_*/M. \tag{2.11}$$

It follows now from (2.7) and (2.8) that

$$nu/z = n_* u_*/z_*, \tag{2.12}$$

$$M \frac{n}{z} u^2 + nT = M \frac{n_*}{z_*} u_*^2 + n_* T_*. \tag{2.13}$$

From this we can express u and n in terms of T and z and the parameters T_* and z_* (which are as yet unknown). Substituting these expressions in (2.9) and (2.10) we obtain the system

$$dz/dx = F(z, T; z_*, T_*), \quad dT/dx = G(z, T; z_*, T_*). \tag{2.14}$$

We are interested in a solution of the system $z(x)$ and $T(x)$ for which

$$z(0) = 0, \quad T(0) = 0. \tag{2.15}$$

The first condition is connected with the fact that near the target the degree of plasma ionization is much less than the mean value. The cause of the second condition is that near the target the kinetic energies of all the plasma particles are of the order of the atomic energy, i.e., much less than the average plasma temperature.

The system (2.14) determines a family of trajectories in the (z,T) plane, along which the x varies. The equation for the trajectories is

$$dT/dz = H(z, T; z_*, T_*), \quad H = G/F. \tag{2.16}$$

The condition (2.15) means that the trajectory corresponding to the sought solution must pass through the point $(0,0)$. At the same time, if z_* and T_* are chosen, the trajectory passing through the point $J = (z_*, T_*)$ is uniquely defined, and it need not necessarily pass through the point $(0,0)$. For this to be the case, it is necessary to impose some connection between z_* and T_*. That this connection is unique follows from the fact that there are three free parameters, z_*, T_*, and x_*, but only two conditions (2.15). The connection between z_* and T_* is indeed the boundary condition for the region of the nonstationary plasma flow mentioned in the Introduction.

3. PHASE PORTRAIT OF THE FORMATION REGION

Let us determine the trajectories of the system (2.14) in the (z,T) plane. It can be seen from (2.10) that in the entire (z,T) plane we have $dT/dx > 0$. We turn now to (2.9); the function γ_z reverses sign on a certain curve C in the (z,T)
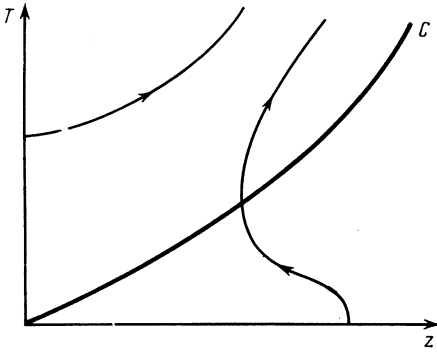
FIG. 1. Characteristics of plasma formation region.

plane; this is the coronal equilibrium curve. Ionization predominates above this curve and $dz/dx > 0$, while recombination predominates below and $dz/dx < 0$. We thus have $dT/dz > 0$ above C and dT/dz below, while on the curve C itself $dT/dz = \infty$.

If $T \to 0$, it can be seen by using (1.7) and (1.12) that $H \sim T^{-2} \to \infty$. It can be seen from these same expressions that if $z \to 0$ then $H \sim z^{k+1} \to 0$. In other words, $dT/dz = \infty$ on the z axis and $dT/dz = 0$ on the T axis.

Bearing the foregoing in mind, we can construct the typical characteristics shown in Fig. 1. In particular, it is clear from the figure that the point J cannot lie below C, for then the trajectory arrives at J from the region $z > z_*$ instead of from the region $z \approx 0$.

Let us see how the character of the trajectories changes with change in thermal conductivity.

Let $x \to \infty$. We then have $dT/dz \approx 0$ everywhere except in a small vicinity of the curve C and a small vicinity of the z axis. The characteristics will have the form shown in Fig. 2a. All the characteristics departing from the region of small z and T "hug" the curve C, so that this curve, near which the point J is located, can be taken to be the sought trajectory. In this case the boundary condition is

$$\gamma_{\bar{z}}(z_*, T_*) = 0.$$

This is physically obvious. If x is increased, to maintain the heat flux constant we must increase the formation-region thickness x_*. The time of flight of the plasma through this region is then increased enough for ionization-recombina-
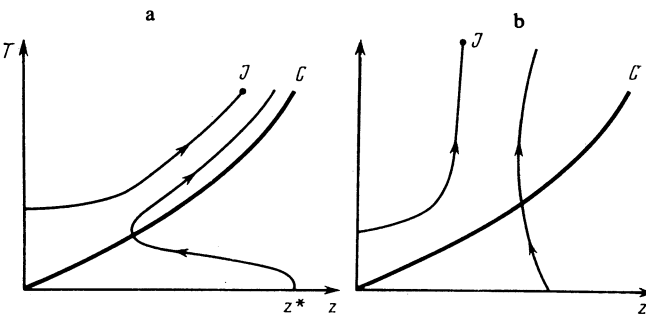

FIG. 2. Characteristics of plasma formation region in the case of high (a) and low (b) thermal conductivity of the plasma.

tion equilibrium to be established in this region. This is precisely the circumstance described by the fact that the characteristic hugs the equilibrium curve.

Let now $x \to 0$. We then have $dT/dz \to \infty$ everywhere except in a small vicinity of the T axis. Characteristics of this type are shown in Fig. 2b. Now the charcteristics departing from the region of small z and T move abruptly upward and it is clear that a noticeable degree of ionization z will be reached only far above the curve C. This means that the recombination can be completely neglected. In this case the plasma is not fully ionized, i.e., z_* is smaller than the degree of ionization at the temperature T_*.

4. BOUNDARY CONDITION FOR PLASMA JET

The solution program indicated in Sec. 2 is most conveniently carried out by transforming to the dimensionless variables

$$N = n/n_*, \quad s = u/u_*, \quad \theta = T/T_*, \quad \zeta = z/z_*. \tag{4.1}$$

In these variables, Eqs. (2.12) and (2.13) take the form

$$Ns = \zeta, \quad s + N\theta = 2. \tag{4.2}$$

Hence

$$s = 1 \pm (1 - \zeta\theta)^{1/2}, \tag{4.3}$$

$$N = (2 - s)/\theta. \tag{4.4}$$

The necessary solution is chosen from the following considerations. In order for absorption to take place actually at the point x_* it is necessary that at $x < x_*$ (i.e., between the target and the critical point) we have $n > n_*$, i.e., $N > 1$. If we choose for s the solution with the minus sign, then on going from $x = 0$ to $x = x_*$ the value of s increases from zero to unity, since ζ and θ increase from zero to unity, in accord with the meaning of the problem. Since both s and θ increase with increasing distance from the target, N decreases to $N = 1$ at $x = x_*$, thus ensuring satisfaction of the condition $N > 1$.

We have thus

$$s = 1 - (1 - \zeta\theta)^{1/2}, \tag{4.5}$$

$$N = [1 + (1 - \zeta\theta)^{1/2}]/\theta, \tag{4.6}$$

i.e., now s and N are known functions of ζ and θ.

We now rewrite (2.16) in the dimensionless variables and confine ourselves to the case when the recombination is negligible. This is done as follows. We transform in (2.9) and (2.10) to the dimensionless variables and separate these equations. We express next the resultant parameters u_*, T_*, and z_* in terms of the parameters β_* and ε defined as follows:

$$\beta_* = E_{z_*}/T_* = (E_0/T_*)z_*^k = \varepsilon^{-1}z_*^k, \tag{4.7}$$

$$\varepsilon = T_*/E_0. \tag{4.8}$$

In addition, we introduce a parameter that describes the target,

$$\lambda = Mx_0S_0/3E_0. \tag{4.9}$$

The values of M and λ for different ions are given in Table I. The indicated transformations yield

$$d\theta/d\zeta = q\varphi(\xi)\chi(\beta),\tag{4.10}$$

where we have introduced the functions

$$\chi(\beta) = \beta^{(k+2)/(k+1)}e^\beta(\beta+a),\tag{4.11}$$

$$\varphi(\xi) = {}^1\!/_6\,\xi^{-k/(k+1)}s^2(s^2+5\xi),\tag{4.12}$$

which depend on the variables

$$\beta = \beta_*\theta^{-1}\zeta^k,\quad \xi = \theta\zeta.\tag{4.13}$$

Since the calculations are semi-quantitative, the exact value of γ is not very important, and we assume $\gamma = 5/3$. The parameter q is independent of ζ and θ and is defined as

$$q = \lambda^{-1}\varepsilon^{3/k}\beta_*^{(2k+3)/k(k+1)}.\tag{4.14}$$

The right-hand side of (4.10) contains, besides the variables ζ and θ, the two parameters q and β_*. The condition for the existence of a trajectory that connects the points $(0,0)$ and $(1,1)$ in the (ζ,θ) plane yields the connection between q and β_*, i.e., according to (4.14), the connction between ε and β_*. Substituting here (4.7) and (4.8), we obtain the sought connection between T_* and z_*.

It will be made clear below that the experimental conditions correspond to $q \ll 1$. We consider therefore only this case. An analysis of (4.10) at small q shows that the trajectories of interest to us, which arrive in the vicinity of the point $(\zeta = 1, \theta = 1)$ from the region of small ζ and θ, lie close to the curve $\beta = \beta_*$, i.e., near the parabola $\theta = \zeta^k$. These trajectories are shown in Fig. 3. It can be approximately assumed that the trajectory leaving the point $(\zeta = 0, \theta = 0)$ and arriving at the point $(\theta = 1, \zeta = 1)$ coincides with the parabola $\theta = \zeta^k$. In this approximation, the derivative along the trajectory at the critical point is

$$(d\theta/d\zeta)_{\zeta=1,\,\theta=1} = k.\tag{4.15}$$

It follows from (4.15) and (4.10) that
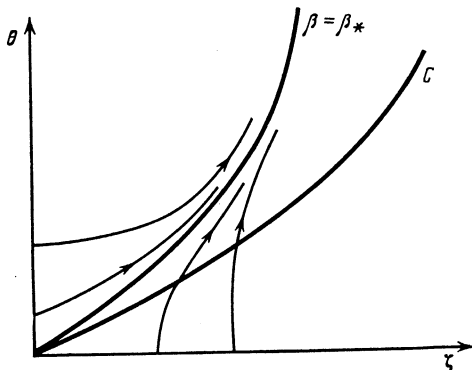
$$q\chi(\beta_*) = k.\tag{4.16}$$

FIG. 3. Characteristics of the plasma formation region at $q \ll 1$.

This indeed is the sought connection between q and β_* at small q. Returning to the variables ε and β_*, we can rewrite (4.16) in the form

$$\frac{1}{k}\varepsilon^{3/k}\beta_*^{3/k+2}e^{\beta_*} = \lambda.\tag{4.17}$$

In the derivation of (4.17) we have neglected the quantity $a \lesssim 1$ in (4.11). This is correct if $\beta \gg 1$. We note that the condition $\beta \gg 1$ follows from (4.16) at $q \ll 1$, inasmuch as the typical values of k are close to unity.

Equation (4.17) is the sought boundary condition that connects the temperature T_* with the degree z_* of the plasma ionization on the boundary of the region of formation of the plasma and the plasma jet. This equation contains the parameters of the plasma and of the target (via λ, E_0, and k), but not the radiation power. We show one more form, sometimes more convenient, of the boundary condition,

$$z_*^3\beta_*^2e^{\beta_*} = k\lambda,\tag{4.18}$$

which is obtained from (4.17) by expressing ε in terms of β_* and z_* with the aid of (4.7). The proximity of the trajectory to the $\beta = \beta_*$ curve means that in the region of plasma formation the ratio E_z/T is a (large) constant.

We now obtain the ionization and temperature profiles. We transform over in (2.9) to the dimensionless variables and integrate along the trajectory from $x = 0$ to a certain arbitrary x. Noting that this integration $\beta = \beta_*$ and $\theta = \zeta^k$, we obtain after simple transformations

$$x = \frac{u_0}{n_*S_0}z^{2k+\frac{5}{2}}\,e^{\beta_*}I_k(\zeta),\tag{4.19}$$

where

$$I_k(\zeta) = \int_0^\zeta d\zeta\,\zeta^{5k/2}\frac{1-(1-\zeta^{k+1})^{\frac{1}{2}}}{1+(1-\zeta^{k+1})^{\frac{1}{2}}},\tag{4.20}$$

$$Mu_0^2 = E_0.\tag{4.21}$$

Equation (4.19) determines the function $\zeta(x)$, i.e., the ionization profile. The temperature profile is $\theta(x) = \zeta^k(x)$. We put in (4.19) $x = x_*$ and $\zeta = 1$, and use the boundary condition (4.18), in order to express z_* in terms of β_*. As a result we obtain the thickness of the formation region

$$x_* = k^{(4k+3)/6}I_k(1)\frac{u_0}{n_*S_0}\lambda^{(4k+3)/6}\beta_*^{-(4k+3)/3}\,e^{-(4k-3)\beta_*/6}.\tag{4.22}$$

The integral $I_k(\zeta)$ was obtained by numerical integration for the value $k = 1.4$, which is typical of the 2s–2p shells of the ions from Ca to Cu (see Table I). Figure 4 shows the profiles of the ionization, temperature, electron density, and gasdynamic-flow velocity of the plasma. It must be noted that the derivative of the electron density with respect to the coordinate, $\partial n/\partial x$, and the acceleration, $du/dt = u_*^2s\partial s/\partial x$, are infinite at the critical point. As indicated in Ref. 2, this is due to the assumption of a δ-like absorption of the laser radiation on the critical surface.

We note that a degree of polarization amounting to 0.9 of the maximum is reached at a distance $0.35x_*$.
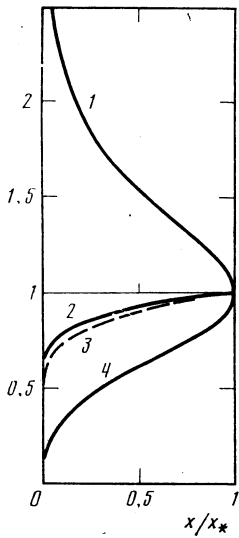
FIG. 4. Profiles of the degree of ionization z/z_* (curve 2), the temperature T/T_* (curve 3), the density n/n_* (curve 1), and the velocity u/u_* (curve 4) of the thermodynamic flux in the formation layer.

It follows from Table IV below that the characteristic values x_* lie in the range $10 \leqslant z_* \leqslant 20$. For these z_*, at temperatures T_* from 150 to 500 eV, the parameter β_* ranges from 4 to 2 (see Table III). In this case q takes on values $0.01 - 0.2$. Although q is indeed small, typical values of β_* are not very large. This is due to the exponential factor $e^{\beta}*$ in (4.16). The error due to neglecting a in (4.11) can therefore reach 30%, since $a \lesssim 1$. A much better accuracy could be obtained by investigating the phase portrait numerically.

Let us estimate also, using Ca as an example, the role of recombination, by comparing the terms in the curly brackets of (1.5). For Ca we have $b \approx 0.5$ and $r \approx 0.8 \times 10^{-6}$ according to Ref. 4, so that in the considered region of the parameters the first term is of the order of 10^{-2}, and the second of 10^{-4}, i.e., the recombination is indeed insignificant. This conclusion follows also from the plots given in Ref. 7 for the ionization equilibrium with account taken of dielectron recombination. It is seen from them, for example, that at $T = 2.50$ eV $= 2.9 \times 10^6$ K the fraction of ions with $z = 11$ is less than 1% and ions with large z predominate. This means that at these temperatures recombination is insignificant for ions with $z = 11$.

5. DEPENDENCE OF THE TEMPERATURE AND DEGREE OF IONIZATION OF THE PLASMA ON THE GASDYNAMIC POWER OF THE PLASMA JET

To find the distribution of the temperature and of the degree of ionization of the plasma over the jet, we must solve the equation that describe the plasma expansion, with the boundary condition (4.18). However, the temperature and degree of ionization in the base of the jet (i.e., at the location of its junction with the formation region) can be obtained only by knowing the total gasdynamic power of the jet. The gasdynamic flux W can be obtained by calculating it at the section x_*; using (2.11), we obtain

$$W = \frac{n_*}{z_*} M u_* \left[\frac{1}{2} u_*{}^2 + \frac{5}{2} z_* \frac{T_*}{M} \right] = 3 n_* T_*^{5/2} z_*^{1/2} M^{-1/2}. \tag{5.1}$$

We express T_* in terms of β_*; we introduce the characteristic flux

$$W_0 = 3 n_* E_0 u_0 \tag{5.2}$$

and the dimensionless parameter $w = W/W_0$. We have then from (5.1)

$$w = z_*^{(3k+1)/2} \beta_*^{-7/2}. \tag{5.3}$$

This equation together with (4.18) comprises a system from which we can, given W, obtain z_* and β_* and then find ε, i.e., T_*, with the aid of (4.7). Eliminating z_* from this system, we obtain an equation for determining β_* from w:

$$\beta_*^{(6k+11)/(3k+1)} e^{\beta_*} = k \lambda w^{-6/(3k+1)}. \tag{5.4}$$

Having obtained from this β_*, we calculate z_* and T_* from the formulas

$$z_* = w^{2/(3k+1)} \beta_*^{3/(3k+1)}, \tag{5.5}$$

$$T_* = E_0 w^{2k/(3k+1)} \beta_*^{-1/(3k+1)} \tag{5.6}$$

By reducing the calculation results we can obtain simple power-law relations that connect T_*, z_*, x_*, and u_* with the gasdynamic flux W_*, namely

$$A_*{}^i = A_0{}^i (W/10^{12} \text{ W/cm}^2)^{\alpha_i}, \tag{5.7}$$

where the values $i = 1, 2, 3, 4$ correspond to T_* (keV), z_*, x_* (μm) and u_* (cm/sec). The values of A_0^i and α_i for ions from Ti to Cu are given in Table II. Table III gives the values of z_*, T_* and W calculated at different β_* for Ca in the case

TABLE II.

| i | Ti | | | | Fe | | Ni | | Cu | | | |
| | 2s—2p | | (2s—2p) + + (3s—3p) | | 2s—2p | | 2s—2p | | 2s—2p | | 3s—3p | |
	$A_0{}^i$	α_i	$A_0{}^i$	α_i	$A_0{}^i$	α_i	$A_0{}^i$	α_i	$A_0{}^i$	α_i	$A_0{}^i$	α_i
1	0.25	0.57	0.25	0.61	—	—	—	—	—	—	—	—
2	13.4	0.28	13.5	0.16	13.3	0.28	13.2	0.28	13.4	0.27	18.9	0.30
3	5.2	0.71	9.3	0.98	—	—	—	—	—	—	—	—
4	0.82	0.43	0.83	0.39	—	—	—	—	—	—	—	—

TABLE III.

	I=21 eV $(z+1)^{1,4}$				I=2 eV $(z+1)^{2,3}$			
β_*	z_*	T_*, eV	W. W/cm^2		β_*	z_*	T_*, eV	W. W/cm^2
2.50	18.2	448	$3.0 \cdot 10^{12}$		2.75	18.2	500	$3.5 \cdot 10^{12}$
2.75	15.7	333	$1.8 \cdot 10^{12}$		3.00	15.8	333	$1.8 \cdot 10^{12}$
3.00	13.6	251	$1.1 \cdot 10^{12}$		3.25	13.8	226	$0.94 \cdot 10^{12}$
3.25	11.9	192	$0.7 \cdot 10^{12}$		3.5	12.1	156	$0.5 \cdot 10^{12}$

when only the $2s$–$2p$ shell is taken into account and in the case of averaging over the $2s$–$2p$ and $3s$–$3p$ shells.

It can be seen from Tables II and III that in both approximations the values of T_* and z_* are the same at $W = 10^{12}$ W/cm^2. When two shells are taken into account, however, the $z_*(W)$ is less steep, and the thickness of the formation is approximately doubled.

6. EXPERIMENT

We have irradiated bulk flat targets of different materials, in vacuum, by pulses of energy from 1 to 15 J and duration 2.5 nsec from a 1.06-μm neodymium-glass laser. The focused-spot diameters ranged in the different cases from 100 to 1500 μm. The density of the multiply charged ions in the produced plama was determined from the emission spectra of those ions which were registered in a direction parallel to the target plane. The spectra were obtained with a spatial resolution along the direction normal to the target, and without a temporal resolution. The Ti and Cu plasmas were investigated with the aid of the spectra in the x-ray region, while the Fe and Ni plasmas were investigated in the vacuum ultraviolet region.

A Johann-type spectrograph with a KHP crystal, circularly bent at a radius 150 mm, was placed in a vacuum chamber. The target was inside the spectrograph. The wavelength region in which the spectra of Li-like and Ne-like ions were observed was 15–25 Å. UF-VR x-ray film was used for the photography. The arrangement of the spectrograph and the experimental setup are similar to those described in Refs. 8 and 9.

We determined from the spectrograms the relative intensities of the spectral lines corresponding to transitions of like type in the shells of the different ions, which yielded in turn the relative densities of the ions with different charges. Account was taken of the fact that in a number of cases these lines are optically thick. The necessary probabilities of the radiative transitions and rates of excitation by electron impact were calculated in accord with Ref. 4. From the relative ion densities we obtained the average charge of the plasma

ions. The spectra of the multiply charged Ca, Fe, and Ni ions in the 80–200 Å range were registered with a glancing-incidence vacuum spectrograph ($R = 1$ m, $\rho = 600$ lines/mm, $\alpha = 8°$), equipped with a gold-coated grating. The average charge was determined from the spectral lines corresponding to the transitions between the configurations $2s2p^{m+1}$ and $2s^2 2p^m$ ($m = 5 - 0$), which are characterized by small optical thicknesses ($\tau < 1$ or $\tau \approx 1$ for the most intense lines). The registration of the vacuum-ultraviolet spectra with spatial resolution is described in Ref. 10.

In some cases (see e.g., Ref. 11), we tracked the behavior of the ion composition of the plasma with increasing distance from the target. It was found that, at least startig with distances 50–100 μm, the ion composition remains practically unchanged with further expansion of the plasma.

The spatial resolution of our spectrograms was mainly approximately 50 μm. We were therefore unable to measure directly the ion composition at the critical point. The experimental values z_e of the average ion charge, given in Table IV and in Fig. 5, correspond to a distance 50–100 μm from the target surface. The described "freezing" of the ion composition in the expanding plasma, due to the rapid decrease of the plasma electron density and plasma temperature, should make these values of z_e close to those at the critical point.

The experimental values of the average plasma ion charge are compared in Table IV with the theoretical ones calculated from Eqs. (5.7) with the parameters from Tables II and III. In individual cases, to reconcile the theoretical results with the experimental ones a coefficient $\eta = W/P$ was introduced for the conversion of the laser radiation flux P into the gasdynamic flux W. Figure 5 shows the experimental dependence of the average charge z on the laser radiation flux incident on the target for a titanium plasma and the theoretical dependence calculated under the assumption that the total laser-radiation energy was converted into the gasdynamic flux ($\eta = 1$).

It can be seen from the figure and from Table IV that the theoretical values agree well with experiment at laser-radiation fluxes $P \approx 10^{12}$ W/cm^2. At larger fluxes, the theoretical

TABLE IV.

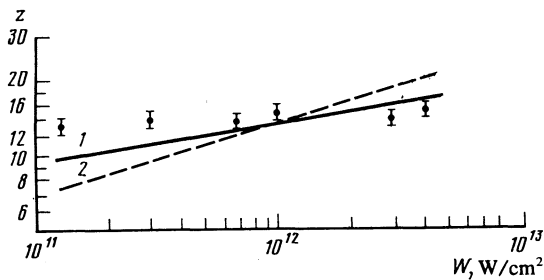|	Ca			Fe			Ni		Cu
P, W/cm^2	$(3-4.5)\cdot 10^{11}$	$(1-1.5)\cdot 10^{13}$		$4\cdot 10^{11}$	$(1-1.5)\cdot 10^{13}$		$(1-1.5)\cdot 10^{13}$		$1.2\cdot 10^{12}$
z_e	12.5	13.5		16.5	19.5		20		20.4
$\eta = W/P$	1	1	0.1—0.07	1	1	0.27—0.40	1	0.3—0.45	1
z_{*T}	9.5 — 10.7	17	13.5	14.4	23	19.5	24.9	20	18

FIG. 5. Average charge z vs gasdynamic flux W for a tantalum plasma: curve 1—averaging over the $2s$–$2p$ and $3s$–$3p$ shells, 2—averaging over the $2s$–$2p$ shell only; ●—experimental points—average charge vs laser radiation flux density (P) for a titanium plasma.

values of $\bar{z}$ exceed the experimental ones and the theory can be reconciled with experiment by introducing $\eta < 1$. At small values of P, the theory leads to smaller vlaues of $\bar{z}$ than experiment. In Fig. 5, the theoretical plot determined for titanium-plasma parameters averaged over the $2s$–$2p$ and $3s$–$3p$ shells ($k = 3.2; E_0 = 0.22$ eV) describes the experimental results better than in the case when only one shell is taken into account.

We note also that measurements of the electron temperature T_e, carried out in Ref. 8 at a laser ($\lambda = 1.06 \mu$m) flux $P = (5-7) \times 10^{12}$ W/cm^2 at the target, yielded a value $T_e = 350$ eV, which is also quite close to the theoretical calculations.

When comparing theory and experiment, the following must be borne in mind. The value of z_e is an average over the jet and may not be equal to z_*, but the two should be close, all the more since the experiment points to "freezing" of the ionization in the course of the expansion.

There is also some uncertainty in the definition of the power P. It can be assumed, of course, that $W = P$, since the energy consumed in evaporation and ionization of the plasma is low. In fact, we shall assume a pulse energy $Q = 10$ J and an evaporated mass (of a calcium target) equal to 10^{-8} g (evaporation rate 400 Å/nsec at a pulse duration 2.5 nsec and a focal spot area 4×10^4 cm^2; the target density is 2.8 g/cm^3). The number of evaporated molecules is then 8×10^{13}, and the number of electrons produced upon ionization is $8 \times 10^{13} \times 13 \approx 10^{15}$. Assuming that 700 eV are needed for each ionization act, we find that the energy consumed by ionization is 0.1 J. Obviously, the evaporation energy is even less. If, however, we start from the measured plasma-expan-sion rate $u = 4.4 \times 10^7$ cm/sec, the kinetic energy of the dispersing particles is approximately 1 J. In other words, the gasdynamic flux W can be also much less than the laser P (for example, on account of losses to reflection).

At the same time, the calculations presented are also quite approximate. There are several sources of errors. For example, there is no full confidence in the values of the ionization probabilities S_z, especially for the $3s$–$3p$ shell, where we have assumed the parameters A and a to be the same as in the $2s$–$2p$ shell. Many inaccuracies are introduced by the "analytical" method of the calculation; the condition $\beta_* \gg 1$ is not very well satisfied; the impossibility of joining the shells leads to overestimates of z_* at the start of the shell ionization if the parameters of the preceding shell is used, and to undervalued z_* at the end of the shell ionization, since the ionization potentials of the preceding shell are overestimated. Taking all the foregoing into account, it must be conceded that in the absence of fit parameters the agreement between the theoretical calculations and the experiment is fair.

[1]Yu. V. Afanas'ev, E. G. Gamaliĭ, L. N. Krokhin, and V. B. Rozanov, Zh. Eksp. Teor. Fiz. **71**, 594 (1976) [Sov. Phys. JETP **44**, 311 (1976)].
[2]Yu. V. Afanas'ev, N. G. Basov, O. N. Krokhin, V. V. Pustovalov, V. P. Silin, G. V. Sklizkov, V. T. Tikhonchuk, and A. F. Shikanov, in: Radiotekhnika (Radio Engineering), N. G. Basov, ed., Vol. 17, VINITI, 1978, p. 81.
[3]S. I. Anisimov, Ya. A. Imas, G. S. Romanov, and Yu. I. Khodyko, Deĭstvie izlucheniya bol'shoĭ moshchnosti na metally (Effect of High-Power Radiation on Metals), Nauka, 1970, §4.1.
[4]L. A. Vainshtein, I. I. Sobel'man, and E. A. Yukov, Secheniya vozbuzhdeniya atomov i ionov élektronami (Cross Sections for Excitation of Atoms and Ions by Electrons), Nauka, 1973.
[5]R. L. Kelly and L. J. Palumbo, Atomic and Ionic Emission Lines below 2000 Angstroms, NRL Report 7599, Washington, 1973.
[6]L. Spitzer, Physics of Fully Ionized Gases, Wiley, 1962.
[7]I. L. Beĭgman, A. A. Vainshtein, and R. A. Syunyaev, Usp. Fiz. Nauk **95**, 267 (1969) [Sov. Phys. Usp. **11**, 411 (1969)].
[8]G. V. Peregudov, E. N. Ragozin, and V. A. Chirkov, Kvant. Elektron. (Moscow) **2**, 1844 (1975) [Sov. J. Quantum Electron **5**, 1012 (1975)].
[9]V. I. Bayanov, S. S. Guludov, A. A. Mak, G. V. Peregudov, I. I. Sobel'man, A. D. Starikov, and V. A. Chirkov, *ibid.* **3**, 2253 (1976) [7, 1226 (1976)].
[10]A. A. Ilyukhin, G. V. Peregudov, and E. N. Ragozin, *ibid.* **4**, 607 (1977) [7, 336 (1977)].
[11]E. N. Ragozin, *ibid.* **7**, 868 (1980) [10, 493 (1980)].

Translated by J. G. Adashko